Metal–Organic Polyhedra

International Edition: DOI: 10.1002/anie.201503095
German Edition: DOI: 10.1002/ange.201503095

Cooperative Crystallization of Heterometallic Indium–Chromium Metal–Organic Polyhedra and Their Fast Proton Conductivity**

Quan-Guo Zhai, Chengyu Mao, Xiang Zhao, Qipu Lin, Fei Bu, Xitong Chen, Xianhui Bu, and Pingyun Feng**

Abstract: *Metal–organic polyhedra (MOPs) or frameworks (MOFs) based on Cr^{3+} are notoriously difficult to synthesize, especially as crystals large enough to be suitable for characterization of the structure or properties. It is now shown that the co-existence of In^{3+} and Cr^{3+} induces a rapid crystal growth of large single crystals of heterometallic In-Cr-MOPs with the $[M_8L_{12}]$ ($M = In/Cr$, $L =$ dinegative 4,5-imidazole-dicarboxylate) cubane-like structure. With a high concentration of protons from 12 carboxyl groups decorating every edge of the cube and an extensive H-bonded network between cubes and surrounding H_2O molecules, the newly synthesized In-Cr-MOPs exhibit an exceptionally high proton conductivity (up to 5.8×10^{-2} S cm^{-1} at 22.5 °C and 98 % relative humidity, single crystal).*

Metal–organic frameworks (MOFs)[1] (or more generally coordination polymers, CPs[2]) and hydrogen-bonded frameworks including recently developed hydrogen-bonded organic frameworks (HOFs)[3] have emerged as a new promising class of materials that are capable of fast ion conductivity. Their high crystallinity and open framework architecture, together with tunable compositions and structures, make it possible to not only better design materials to optimize ion conduction carriers and pathways, but also better understand conducting behaviors and mechanisms.[4,5]

Highly proton-conducting materials are essential in many applications, especially hydrogen fuel cells. For MOF materials, recently reported strategies for enhancing the proton conductivity have focused on increasing the concentration of proton carriers by controlling framework or extra-framework compositions as well as on improving proton mobility by constructing materials with desired H-bonded networks. For example, Kitagawa et al. reported highly proton-conductive zinc oxalate MOFs by maximizing the proton carriers with the simultaneous introduction of adipic acid molecules on the framework and the counter cation $(NH_4)^+$ in the void space.[6] Another example is PCMOF2$^1/_2$ reported by Shimizu et al.[7] which combined trisulfonate and triphosphonate groups and had conductivity over 0.01 S cm^{-1}.

The design strategy for the synthesis of MOFs can vary significantly depending on the intended applications. For developing better proton conductors, the conventional strategy targeting extended 1D, 2D, or 3D frameworks may not always be desirable. This is because a higher dimensional structure generally requires a greater degree of ligand deprotonation, which necessarily reduces the proton concentration. For this reason, we expect that discrete metal–organic polyhedra (MOPs) that can be formed through partial deprotonation of ligands might represent a promising source of materials capable of improved fast proton conductivity. The finite polyhedral structures of MOPs provide an opportunity to decorate the entire surface with organic ligands that carry extra functional groups so that a higher concentration of proton carriers can be achieved. Moreover, the extensive hydrogen bonding between the MOPs and the surrounding guest molecules could provide an efficient pathway for proton conduction. Prior to this study, even though MOPs have been explored for their potential applications in catalysis, chemical sensing, drug delivery, and separation[8–10] and as building blocks in the construction of extended MOFs or CPs, their proton conducting properties remained little explored.

Compared to complexes based on other metal ions such as Cu^{2+}, Zn^{2+}, and In^{3+}, metal complexes based on Cr^{3+} tend to have long lifetimes with very slow ligand exchange rates. As a result, the synthesis of Cr^{3+} MOPs or MOFs, especially the growth of large-enough single crystals suitable for conventional X-ray diffraction analysis, is among the most difficult tasks in the development of new MOPs and MOFs. In this study, we discovered for the first time that the presence of In^{3+} can induce the crystallization of otherwise non-crystallizable Cr^{3+} MOPs. Specifically, a mixture of In^{3+} and Cr^{3+} can cooperatively crystallize into heterometallic MOPs with high proton conductivity. This strategy opens a new way for creating new Cr^{3+}-based MOFs and also provides a fresh route for the creation of novel fast proton conductors.

In the new MOPs, $[Cr_4In_4(Himdc)_{12}]\cdot H_2O$ (denoted CPM-103a) and $[Cr_{7.28}In_{0.72}(Himdc)_{12}]\cdot H_2O$ (denoted CPM-103b, imdc = 4,5-imidazoledicarboxylate) reported here, a high proton concentration that is due to an abundance of carboxylic acid groups on the surface of each cube (one on each edge for a total of 12 COOH groups per cube), together

[*] Dr. Q. G. Zhai, C. Mao, Dr. X. Zhao, Dr. Q. Lin, F. Bu, X. Chen, Prof. Dr. P. Feng
Department of Chemistry, University of California
Riverside, CA 92521 (USA)
E-mail: pingyun.feng@ucr.edu
Homepage: http://research.chem.ucr.edu/groups/feng/
Prof. Dr. X. Bu
Department of Chemistry and Biochemistry, California State University
Long Beach, CA 90840 (USA)
E-mail: xianhui.bu@csulb.edu
Homepage: http://www.csulb.edu/~xbu/

[**] The work is supported by the US Department of Energy, Office of Basic Energy Sciences, Materials Sciences and Engineering Division under award No. DE-FG02-13ER46972.

Supporting information for this article is available on the WWW under http://dx.doi.org/10.1002/anie.201503095.

with the extensive hydrogen bonds around the cube contributed to the high proton conductivity of the material ($5.8\times10^{-2}\,S\,cm^{-1}$ at 22.5 °C and 98% relative humidity or RH, single crystal). The observed proton conductivity is comparable to that of Nafion ($6.3\times10^{-2}\,S\,cm^{-1}$ for Nafion 117 at 60 °C and 95% RH[11]). On the basis of our extensive literature study, for metal coordination compounds such as MOFs, the highest measured number prior to this study is $4.2\times10^{-2}\,S\,cm^{-1}$ at 25 °C and 98% RH, found in an oxalate-based MOF $\{[(Me_2NH_2)_3(SO_4)]_2\text{-}[Zn_2(ox)_3]\}_n$ (Supporting Information, Table S2).[5a,12]

Large red cube-shaped heterometallic In-Cr-MOP (CPM-103a) single crystals crystallizing in the cubic $Fm\bar{3}c$ space group were synthesized by reacting $Cr(NO_3)_3\cdot9H_2O$, $In(NO_3)_3\cdot xH_2O$, and H_3imdc in the DMF/H_2O (4:1 mass ratio) mixed solvent at 100 °C (Supporting Information). The phase purity of the bulk sample was confirmed by matching the powder X-ray diffraction (PXRD) patterns of In-Cr-MOPs and the PXRD patterns simulated from single crystal analysis (Supporting Information, Figure S4).

When $[Cr_3(\mu_3\text{-}O)(\mu\text{-}CH_3COO)_6(H_2O)_3]NO_3$[13] was utilized instead of $Cr(NO_3)_3\cdot9H_2O$ under the same reaction condition, another In–Cr–MOP crystallizing in the rhombohedral $R\bar{3}$ space group (CPM-103b) was obtained. It is worth noting that crystallization of CPM-103a or CPM-103b would only occur when both Cr^{3+} and In^{3+} precursors are present. Experiments with only Cr^{3+} or In^{3+} source under comparable conditions led to either amorphous gel for Cr^{3+} or unidentified polycrystalline powder for In^{3+} (the proposed crystal growth mechanism in Supporting Information). Owing to the large difference in X-ray scattering factors between Cr and In, the Cr/In ratio could be estimated from the occupancy refinement with single crystal X-ray diffraction data and further supported by the EDX analysis (Supporting Information, Figure S1).

X-ray single-crystal structure analysis shows that the structure of CPM-103a consists of $[M_8L_{12}]$ cubes residing at the crystallographic center of symmetry. The vertices of the cube are occupied by 8 metal ions connected in a bidentate fashion by 12 doubly deprotonated $Himdc^{2-}$ bridging ligands (Figure 1a; Supporting Information, Figure S2). Each metal center is coordinated to 3 O and 3 N from 3 different $Himdc^{2-}$ ligands, leading to the facial octahedral coordination geometry. Each $Himdc^{2-}$ ligand bridges together two individual metal centers to give two five-membered rings that are coplanar with the imidazole ring. The M-M-M angles and M–M distances are 90° and 6.3549(1) Å, respectively, indicating the regularity of the cube.

CPM-103b exhibits a slightly distorted cube owing to its two crystallographically unique metal sites and two $Himdc^{2-}$ ligands (Supporting Information, Figure S3). The M-M-M angles range from 88.881(15)° to 90.612(12)°. The M1 site is pure Cr, but the M2 site is determined to be 0.12 In and 0.88 Cr according to the structural refinements. The Cr/In ratio was also supported by the EDX results (Supporting Information, Figure S1).

The In-Cr-Himdc cubes in CPM-103a or 103b are connected edge-to-edge via O–H···O hydrogen bonds between the carboxylate groups and guest H_2O molecules

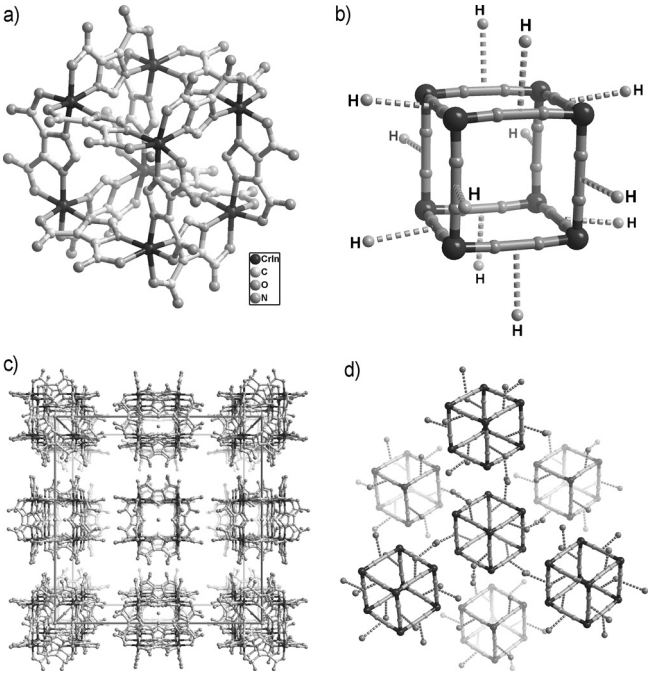

Figure 1. a) Structure of the $[Cr_4In_4(Himdc)_{12}]\cdot H_2O$ cube. b) The distribution of 12 H-atoms on the surface of each cube. c) 3D supramolecular packing of the cubes. d) The orientation of each cube and six neighboring cubes.

to form a pcu (primitive cubic packing) superlattice (Figure 1c; Supporting Information, Figure S3c). As a result, each In-Cr-MOP connects to six neighboring ones (Figure 1d; Supporting Information, Figure S3e). The nearest O···O distances in the same $Himdc^{2-}$ are in the range of 2.9066(1)–3.0533(1) Å, which are markedly longer than the distances commonly observed in the strong hydrogen bonds based on the O···O pairs.[14] Such weakened intramolecular hydrogen bonding is indicative of strong intermolecular hydrogen bonds between the carboxyl groups and guest H_2O molecules, which is believed here to provide efficient pathways for proton conduction.

Samples of CPM-103a and CPM-103b were activated for gas sorption studies by exchanging with CH_3CN for 3 days and then heating at 60 °C for 10 h in a vacuum. Both samples were found to be non-porous to N_2, but exhibited an appreciable CO_2 uptake of 38.8 cm^3g^{-1} and 17.3 cm^3g^{-1} at 273 K and 298 K, respectively (1 atm; Supporting Information, Figure S5). The isosteric heat of adsorption (Q_{st}) of CO_2 was determined by fitting the adsorption data collected at 273 and 298 K to the virial model. CPM-103a and CPM-103b exhibited Q_{st} for CO_2 of 32.2 and 35.4 $kJ\,mol^{-1}$ (Supporting Information, Figure S5), respectively, at zero coverage. These numbers are significantly larger than most of the MOFs and suggest a strong interaction of CO_2 with the surface of MOPs.

To develop materials with enhanced proton conductivity, it can be advantageous to perform synthesis in water-rich solutions owing to the possibility to form extended hydrogen-bonding pathways. Unfortunately, many MOFs or MOPs have limited stability in water. One interesting aspect of CPM-103a and CPM-103b is their crystallization in a water-

rich solvent with 12 carboxyl H atoms around the surface of the MOP, which makes it a potential candidate for proton-conducting material. Also, the availability of large single crystals of CPM-103a makes it possible to investigate the conductivity free from the grain boundary effect.

A single-crystal conductivity measurement was performed on a cube-shaped crystal (0.25 mm × 0.25 mm × 0.25 mm) with the electrodes attached by gallium metal.[15] AC impedance measurement was performed in an incubator at 22.5 °C under various relative humidity (RH). At 45 % RH, the conductivity of CPM-103a was found to be 1.7×10^{-3} S cm^{-1}. Its conductivity increased to 8.0×10^{-3} S cm^{-1} at 75 % RH and reached a maximum value of 5.8×10^{-2} S cm^{-1} at 98 % RH (Figure 2; Supporting Information, Figure S7). In comparison, the conductivity of CPM-103b also shows a humidity dependence, with an increase from 2.3×10^{-4} S cm^{-1} at 45 % RH to 4.8×10^{-2} at 98 % RH (Supporting Information, Figure S8). Furthermore, the reproducible measurements on the same crystal of CPM-103a or 103b between 45 % RH and 98 % RH for 3–4 runs (Supporting Information, Figures S9 and S10) demonstrated the stability of these two MOPs during the impedance measurements.

AC impedance spectroscopy was also performed on a compressed pellet (13 mm in diameter and 3 mm in thickness pelletized at 50 MPa) of the crystalline powder sample. At 98 % RH and 22.5 °C, the proton conductivity reached 2.3×10^{-3} S cm^{-1} and 2.1×10^{-3} S cm^{-1} for CPM-103a and CPM-103b, respectively (Supporting Information, Figures S11 and S12). It was observed that an increased pelletization pressure gave higher proton conductivity values. For samples pelletized at 68 Mp, 6.5×10^{-3} S cm^{-1} for CPM-103a and 5.9×10^{-3} S cm^{-1} for CPM-103b were obtained at 98 % RH and 22.5 °C (Supporting Information, Figure S13, Table S2). The humidity dependence of proton conductivity was also indicated by the Nyquist plots obtained under different humidity conditions (from 45 % to 98 % RH) (Figure 2).

The temperature dependence of the proton conductivity was measured at 93 % RH using a sample (pelletized at 50 MPa) of CPM-103a to further probe the mechanism of proton conduction (Supporting Information, Figure S14). Figure 2c shows the Arrhenius plot of the proton conductivity. The activation energy (E_a) was found to be 0.66 eV, which indicates that the mechanism of proton conduction is expected to be similar to that of the Grotthus mechanism, that is, proton transport from $Himdc^{2-}$ by re-forming hydrogen bonds between $Himdc^{2-}$ and H_2O guest molecules. The E_a value is higher than some well-known hydrated proton conductors, such as PCMOF-5 (0.32 eV)[16], $HUO_2PO_4 \cdot H_2O$ (0.32 eV)[17] and Nafion (0.22 eV);[18] but comparable to inorganic–organic hybrid highly proton-conductive materials, such as $(NH_4)_2$(adipic acid)$[Zn_2(oxalate)_3] \cdot 3H_2O$

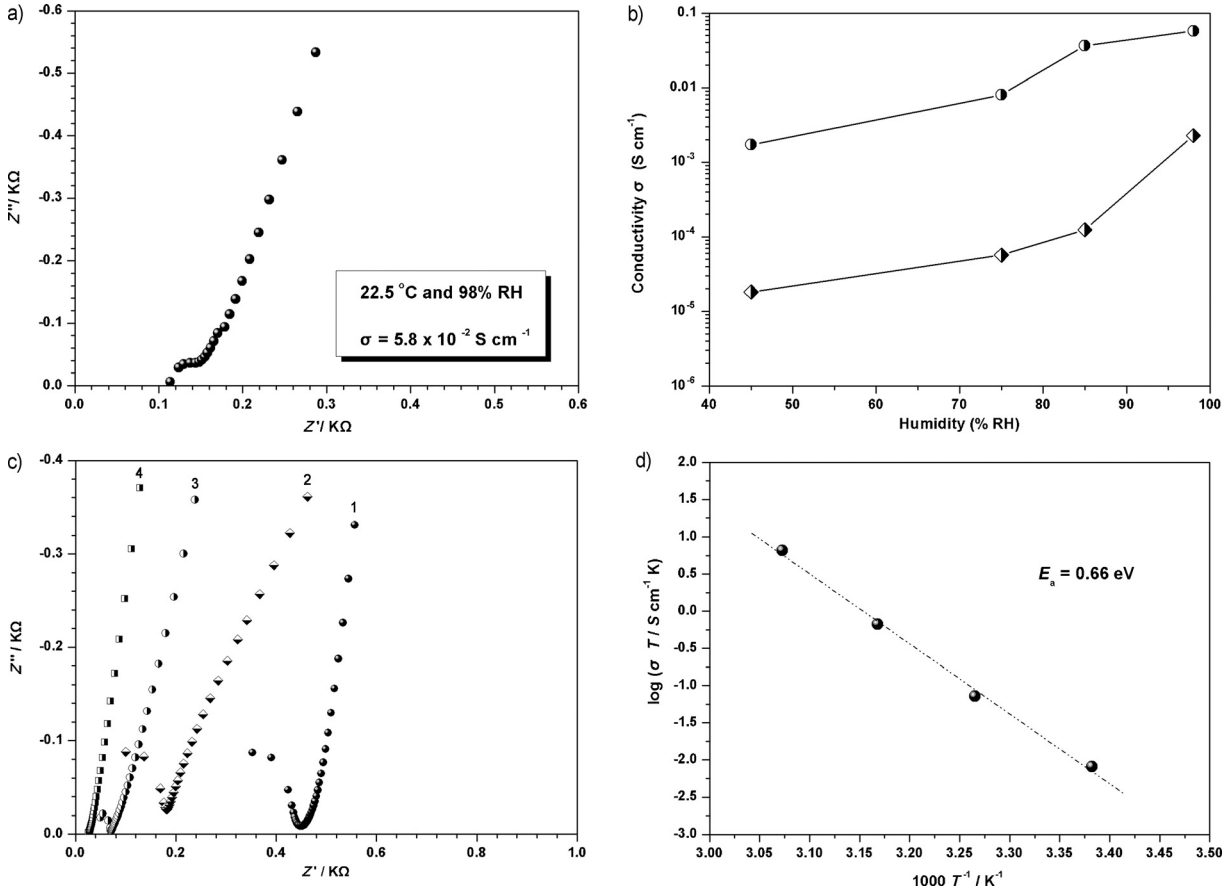

Figure 2. a) Nyquist plot of the single crystal sample of CPM-103a. b) Dependence of the conductivity on humidity of single crystal (upper curve) and pellet samples (lower curve) of CPM-103a. c) Nyquist plots under 93 % RH conditions and different temperatures: 1) 22.5 °C, 2) 33.1 °C, 3) 42.5 °C, 4) 52.3 °C. d) Arrhenius plot of the proton conductivity. Least-squares fitting is shown as a dotted line.

(0.63 eV),[6] In-IA-2D-1(0.61 eV),[19] and {[Ca(D-Hpmpc)-$(H_2O)_2$]·2 $HO_{0.5}$}$_n$/PVP composite (0.65 eV).[20]

In summary, it is demonstrated herein that MOPs have a unique ability to incorporate a high concentration of proton carriers and to establish an extended H-bonded network, which make them promising candidates for proton-conductive materials. We have shown that the incorporation of indium proves to be an effective method to grow Cr^{3+}-based crystals and that the heterometallic In-Cr-MOPs first synthesized here exhibit fast proton conducting behavior. The introduction of high concentrations of proton carriers on the outer surface of the cage and effective pathways for proton conduction via the hydrogen bonds through the guest molecules were found to contribute to the observed high proton conductivity. This research should open up new opportunities for developing promising proton-conductive materials based on MOPs.

Experimental Section

Synthesis of CPM-103a: In a 20 mL glass vial, $In(NO_3)_3 \cdot x H_2O$ (150.0 mg), $Cr(NO_3)_3 \cdot 9H_2O$ (200.0 mg), and 4,5-imidazoledicarboxylic acid (78.0 mg) were dissolved in a mixture of DMF (8.0 g) and water (2.0 g). After the suspension was stirred for 2 h, the vial was sealed and placed in a 100 °C oven for 5 days. Large red cubic crystals were obtained after cooling to room temperature. The yield was about 85 % based on Cr. Pure sample was obtained by filtering and washing the raw product with extra DMF.

Synthesis of CPM-103b: The procedure was similar to that of CPM-103a except 107.0 mg $[Cr_3(\mu_3\text{-}O)(\mu\text{-}CH_3COO)_6(H_2O)_3]NO_3$ was utilized instead of $Cr(NO_3)_3 \cdot 9H_2O$. Large pure red rhombic crystals were obtained with about 80 % yield based on Cr.

Detailed experimental and crystallographic data, figures showing structural details, FTIR spectra, PXRD patterns, TGA curve, gas adsorption isotherms, EDX results, and Nyquist plots are given in the Supporting Information. CCDC 1048262 and CCDC 1048263 contain the supplementary crystallographic data for this paper. These data can be obtained free of charge from The Cambridge Crystallographic Data Centre via www.ccdc.cam.ac.uk/data_request/cif.

Keywords: chromium(III) · cooperative crystallization · indium · metal–organic polyhedra · proton conductivity

How to cite: *Angew. Chem. Int. Ed.* **2015**, *54*, 7886–7890
Angew. Chem. **2015**, *127*, 7997–8001

[1] a) O. M. Yaghi, M. O. Keeffe, N. W. Ockwig, H. K. Chae, M. Eddaoudi, J. Kim, *Nature* **2003**, *423*, 705–714; b) B. Chen, S. Xiang, G. Qian, *Acc. Chem. Res.* **2010**, *43*, 1115–1124; c) J. Yu, Y. Cui, C. Wu, Y. Yang, Z. Wang, M. O'Keeffe, B. Chen, G. Qian, *Angew. Chem. Int. Ed.* **2012**, *51*, 10542–10545; *Angew. Chem.* **2012**, *124*, 10694–10697; d) J. Qin, S. Zhang, D. Du, P. Shen, S. Bao, Y. Lan, Z. Su, *Chem. Eur. J.* **2014**, *20*, 5625–5630; e) H. Fei, D. L. Rogow, S. R. J. Oliver, *J. Am. Chem. Soc.* **2010**, *132*, 7202–7209; f) H. Fei, C. S. Han, J. C. Robins, S. R. J. Oliver, *Chem. Mater.* **2013**, *25*, 647–652; g) S.-T. Zheng, T. Wu, B. Irfanoglu, F. Zuo, P. Feng, X. Bu, *Angew. Chem. Int. Ed.* **2011**, *50*, 8034–8037; *Angew. Chem.* **2011**, *123*, 8184–8187; h) S.-T. Zheng, T. Wu, F. Zuo, C. Chou, P. Feng, X. Bu, *J. Am. Chem. Soc.* **2012**, *134*, 1934–1937; i) S.-T. Zheng, T. Wu, C. Chou, A. Fuhr, P. Feng, X. Bu, *J. Am. Chem. Soc.* **2012**, *134*, 4517–4520; j) S.-T. Zheng, C. Mao, T. Wu, S. Lee, P. Feng, X. Bu, *J. Am. Chem. Soc.* **2012**, *134*, 11936–11939; k) S.-T. Zheng, X. Zhao, S. Lau, A. Fuhr, P. Feng, X. Bu, *J. Am. Chem. Soc.* **2013**, *135*, 10270–10273.

[2] a) S. Kitagawa, R. Matsuda, *Coord. Chem. Rev.* **2007**, *251*, 2490–2509; b) D. Yuan, D. Zhao, D. Sun, H. Zhou, *Angew. Chem. Int. Ed.* **2010**, *49*, 5357–5361; *Angew. Chem.* **2010**, *122*, 5485–5489; c) X. Zhao, F. Liu, L. Zhang, D. Sun, R. Wang, Z. Ju, D. Yuan, D. Sun, *Chem. Eur. J.* **2014**, *20*, 649–652; d) Y. Hu, W. M. Verdegaal, S. Yu, H. Jiang, *ChemSusChem* **2014**, *7*, 734–737; e) H. Jiang, D. Feng, T. Liu, J. Li, H. Zhou, *J. Am. Chem. Soc.* **2012**, *134*, 14690–14693; f) H. Fei, S. R. J. Oliver, *Dalton Trans.* **2010**, *39*, 11193–11200.

[3] a) P. Li, Y. He, Y. Zhao, L. Weng, H. Wang, R. Krishna, H. Wu, W. Zhou, M. O'Keeffe, Y. Han, B. Chen, *Angew. Chem. Int. Ed.* **2015**, *54*, 574–577; *Angew. Chem.* **2015**, *127*, 584–587; b) P. Li, Y. He, J. Guang, L. Weng, J. C.-G. Zhao, S. Xiang, B. Chen, *J. Am. Chem. Soc.* **2014**, *136*, 547–549; c) J. Lü, C. Perez-Krap, M. Suyetin, N. H. Alsmail, Y. Yan, S. Yang, W. Lewis, E. Bichoutskaia, C. C. Tang, A. J. Blake, R. Cao, M. Schröer, *J. Am. Chem. Soc.* **2014**, *136*, 12828–12831; d) P. S. Nugent, V. L. Rhodus, T. Pham, K. Forrest, L; Wojtas, B. Space, M. J. Zaworotko, *J. Am. Chem. Soc.* **2013**, *135*, 10950–10953; Wojtas, B. Space, M. J. Zaworotko, *J. Am. Chem. Soc.* **2013**, *135*, 10950–10953; e) Y. He, S. Xiang, B. Chen, *J. Am. Chem. Soc.* **2011**, *133*, 14570–14573.

[4] a) W. J. Phang, W. R. Lee, K. Yoo, D. W. Ryu, B. S. Kim, C. S. Hong, *Angew. Chem. Int. Ed.* **2014**, *53*, 8383–8387; *Angew. Chem.* **2014**, *126*, 8523–8527; b) M. Yoon, K. Suh, S. Natarajan, K. Kim, *Angew. Chem. Int. Ed.* **2013**, *52*, 2688–2700; *Angew. Chem.* **2013**, *125*, 2752–2764; c) T. Yamada, K. Otsubo, R. Makiura, H. Kitagawa, *Chem. Soc. Rev.* **2013**, *42*, 6655–6669; d) S.-L. Li, Q. Xu, *Energy Environ. Sci.* **2013**, *6*, 1656–1683; e) S. Horike, D. Umeyama, S. Kitagawa, *Acc. Chem. Res.* **2013**, *46*, 2376–2384; f) H. Okawa, M. Sadakiyo, T. Yamada, M. Maesato, M. Ohba, H. Kitagawa, *J. Am. Chem. Soc.* **2013**, *135*, 2256–2262; g) N. C. Jeong, B. Samanta, C. Y. Lee, O. K. Farha, J. T. Hupp, *J. Am. Chem. Soc.* **2012**, *134*, 51–54; h) A. Shigematsu, T. Yamada, H. Kitagawa, *J. Am. Chem. Soc.* **2011**, *133*, 2034–2036; i) T. Yamada, M. Sadakiyo, H. Kitagawa, *J. Am. Chem. Soc.* **2009**, *131*, 3144–3145.

[5] a) S. S. Nagarkar, S. M. Unni, A. Sharma, S. Kurungot, S. K. Ghosh, *Angew. Chem. Int. Ed.* **2014**, *53*, 2638–2642; *Angew. Chem.* **2014**, *126*, 2676–2680; b) S. Horike, D. Umeyama, M. Inukai, T. Itakura, S. Kitagawa, *J. Am. Chem. Soc.* **2012**, *134*, 7612–7615; c) D. Umeyama, S. Horike, M. Inukai, T. Itakura, S. Kitagawa, *J. Am. Chem. Soc.* **2012**, *134*, 12780–12785; d) M. Sadakiyo, H. Okawa, A. Shigematsu, M. Ohba, T. Yamada, H. Kitagawa, *J. Am. Chem. Soc.* **2012**, *134*, 5472–5475; e) S. C. Sahoo, T. Kundu, R. Banerjee, *J. Am. Chem. Soc.* **2011**, *133*, 17950–17958; f) J. M. Taylor, R. K. Mah, I. L. Moudrakovski, C. I. Ratcliffe, R. Vaidhyanathan, G. K. H. Shimizu, *J. Am. Chem. Soc.* **2010**, *132*, 14055–14057; g) S. Bureekaew, S. Horike, M. Higuchi, M. Mizuno, T. Kawamura, D. Tanaka, N. Yanai, S. Kitagawa, *Nat. Mater.* **2009**, *8*, 831–836; h) D. Umeyama, S. Horike, M. Inukai, Y. Hijikata, S. Kitagawa, *Angew. Chem. Int. Ed.* **2011**, *50*, 11706–11709; *Angew. Chem.* **2011**, *123*, 11910–11913; i) J. A. Hurd, R. Vaidhyanathan, V. Thangadurai, C. I. Ratcliffe, I. L. Moudrakovski, G. K. H. Shimizu, *Nat. Chem.* **2009**, *1*, 705–710.

[6] M. Sadakiyo, T. Yamada, H. Kitagawa, *J. Am. Chem. Soc.* **2009**, *131*, 9906–9907.

[7] S. Kim, K. W. Dawson, B. S. Gelfand, J. M. Taylor, G. K. H. Shimizu, *J. Am. Chem. Soc.* **2013**, *135*, 963–966.

[8] B. Olenyuk, J. A. Whiteford, A. Fechtenkötter, P. J. Stang, *Nature* **1999**, *398*, 796–799.

[9] N. Takeda, K. Umemoto, K. Yamaguchi, M. Fujita, *Nature* **1999**, *398*, 794–796.

[10] J.-R. Li, H.-C. Zhou, *Nat. Chem.* **2010**, *2*, 893–898.

[11] G. H. Li, C. H. Lee, Y. M. Lee, C. G. Cho, *Solid State Ionics* **2006**, *177*, 1083–1090.

[12] During the initial review of this manuscript, a new fast proton conductor ($8.4\times10^{-2}\,S\,cm^{-1}$ at 80 °C and 90% RH) based on a UiO-66 framework functionalized with sulfonic acid groups was reported: W. J. Phang, H. Jo, W. R. Lee, J. H. Song, K. Yoo, B. Kim, C. S. Hong, *Angew. Chem. Int. Ed.* **2015**, *54*, 5142 – 5146; *Angew. Chem.* **2015**, *127*, 5231 – 5235.
[13] T. Fujihara, J. Aonahata, S. Kumakura, A. Nagasawa, K. Murakami, T. Ito, *Inorg. Chem.* **1998**, *37*, 3779 – 3784.
[14] M. H. Alkordi, J. A. Brant, L. Wojtas, V. C. Kravtsov, A. J. Cairns, M. Eddaoudi, *J. Am. Chem. Soc.* **2009**, *131*, 17753 – 17755.
[15] X. Zhao, C. Mao, X. Bu, P. Feng, *Chem. Mater.* **2014**, *26*, 2492 – 2495.
[16] J. M. Taylor, K. W. Dawson, G. K. H. Shimizu, *J. Am. Chem. Soc.* **2013**, *135*, 1193 – 1196.
[17] L. Bernard, A. Fitch, A. F. Wright, B. E. F. Fender, A. T. Howe, *Solid State Ionics* **1981**, *5*, 459 – 462.
[18] G. Alberti, M. Casciola, *Solid State Ionics* **2001**, *145*, 3 – 16.
[19] T. Panda, T. Kundu, R. Banerjee, *Chem. Commun.* **2013**, *49*, 6197 – 6199.
[20] X. Liang, F. Zhang, W. Feng, X. Zou, C. Zhao, H. Na, C. Liu, F. Sun, G. Zhu, *Chem. Sci.* **2013**, *4*, 983 – 992.

Received: April 3, 2015
Published online: May 15, 2015

